

Predicting Land Use/Land Cover Changes in the Lesser Zab River Catchment/Iraq through CA-Markov Synergy Model

Zahra A. Mahdi

The University of Babylon

Ruqayah Mohammed (✉ r.mohammed1@yahoo.com)

The University of Babylon

Research Article

Keywords: Classification, Lesser Zab catchment, Land use/land cover, Likelihood, Urban expansion

Posted Date: September 15th, 2022

DOI: <https://doi.org/10.21203/rs.3.rs-1916300/v2>

License:   This work is licensed under a Creative Commons Attribution 4.0 International License.

[Read Full License](#)

Abstract

Land use/land cover is one of the utmost dynamic constituents of the atmosphere that has been altering abnormally from the time after the industrial revolution at different measures. A good understanding of the drive and strength of environments needs regular monitoring and quantifying for land use/land cover alterations. The current research targets to predict the prospect of land use/land cover (LU/LC) alterations; for the Lesser Zab catchment in the Northern part of Iraq, applying the synergy Cellular Automata-Markov simulation. The Maximum Likelihood method classified three sequential years of Landsat images (1999, 2010, and 2021). Then, three LU/LC images, with numerous class classifications, were created, and an alteration identification examination; was performed. With the categorized (1999–2010) and (2010–2021) LU/LC maps in the hybrid model, the corresponded LU/LC maps; for 2021 and 2041; were modelled, and the classified 2021 LU/LC maps; were considered to validate the model output 2021. In that order, agreement accuracy between the classified and the modelled images was $K_{no} = 0.864$, $K_{location} = 0.854$, and $K_{standard} = 0.785$. Prospect likelihoods validate that between 2021 and 2041, the urban area would rise by 78% (from 1118 to 5200 km²). However, bare lands/light, agricultural lands, water bodies, bare lands/dark, and forest lands would decrease by 3% (from 6983 to 6736 km²), 12% (from 7992 to 7036 km²), 15% (from 141.03 to 119.86 km²), 30% (from 7 to 4 km²), and 76% (from 3810 to 904 km²), correspondingly. This study's conclusions are priceless for policymakers, urban managers, and ecological researchers.

Introduction

Land use/land cover (LU/LC) alteration has become an international problem, causing rising distress among managers and policymakers regarding the potential impact of such change on the environment (Oliver & Morecroft, 2014; Padmaja & Giridhar, 2022). The modelling and prediction of LU/LC change patterns have become essential to the protection of the ecosystem and maintainable improvement (Saleh & Ahmed, 2021). Compared with the past, the LU/LC concentration, quickness, and amount of alteration are currently quicker caused by public development. The fast growth in inhabitants has disturbed the Globe (Saleh & Ahmed, 2021; Mahdi & Mohammed, 2022). Thus, simulating present and prospective LU/LC alteration would be essential to the policy-making of ecological management and future development. Due to their capability to offer recurrent statistics at changed spatiotemporal coverage, there has been raising concern about applying remote sensing (RS) information for observing LU/LC variations. The RS information is considered vital data to the LU/LC classification and modification exposure simulation. Landsat images are freely available, access to four eras of world recording data, and moderately areal resolution, to investigate LU/LC change; were considered (Sakthivel et al., 2021; Shteiwi et al., 2021; Padmaja & Giridhar, 2022). To simulate LU/LC changes patterns, different methodologies, using RS and GIS, were applied (Saleh & Ahmed, 2021). RS and GIS approaches are inexpensive, provide suitable visual analysis, and have updatable spatial and temporal databases. They are helpful tools for aiding planners and policymakers in developing sustainable policies. Consequently, planners and policymakers have recently considered such techniques to simulate LU/LC change patterns.

Currently, different models and strategies, using RS and GIS techniques, are using to simulate LU/LC changes and model broad urban growth trends (Wang et al., 2018). Several researchers have applied conventional models, such as the cellular automata (CA) models and logistic regression (Wang et al., 2018). However, others have depended on linking various models, such as the CA and Markov chain (MC) models, to achieve accurate and realistic results (Wang et al., 2018). The CA model has an open framework and can be linked with other models to simulate and predict LU/LC changes patterns (Wang et al., 2018). Due to its adaptability, intuitiveness, and capacity to combine spatial and temporal dimensions of numerous processes, the model has found extensive use in simulating future LU/LC changes and urban growth patterns. Furthermore, the CA model has a high spatial resolution; and computational efficiency as the model can be linked with the GIS environs (Wang et al., 2018). The Markov chain model is commonly applied to simulate and predict the LU/LC changes pattern (Yi et al., 2022). Although, the Markov chain model cannot predict changes in spatial trends. However, it is still a powerful model and capacity to predict to which extent land has changed (Wang et al., 2018). Incorporating the CA and Markov Chain models is sufficient for modelling spatiotemporal dynamics of LU/LC since equally are GIS and RS models that can be competently combined (Wang et al., 2018). Linking CA, a dynamic simulation model, with a Markov chain, which is a statistical and empirical model, would overcome the inherent shortcomings in each. Markov model and cellular automata have portable profits in the investigation of land use variations. The CA-Markov simulation can incorporate the data of geographic information systems (GIS) and remote sensing well. Therefore, it is a strong and appropriate technique for simulating spatiotemporal change of LU/LC (Wang et al., 2018; Yi et al., 2022). Recently, the CA Markov model has effectively been applied to simulate the spatiotemporal change patterns of LU/LC by numerous studies (Hailu et al., 2018; Gidado et al., 2019; Msofeet al., 2019; Dibaba et al., 2020; Hishe et al., 2020; Munthali et al., 2020; Cui et al., 2021; Wang & Zheng, 2022; Yi et al., 2022). Accordingly, considering the ability of the model to expand understanding of the difficulty of spatial system components, the current study considered the CA-Markov simulation to examine prospect LU/LC variations within Lesser Zab River Catchment (LZRC), north part of Iraq. During the past decades, LU/LC in Iraq has been harmfully affected by the anthropogenic intervention and climate changes, such as wars and droughts (UN, 2013). A comprehensive estimation of LU/LC in the country is unavailable, and the formal Iraqi administration data may be undependable (Khwarahm et al., 2021a). Nevertheless, numerous studies have used classification methods that are founded on remote sensing data to estimate LU/LC at the local scale (Degife et al., 2019; Juliev et al., 2019; Yesuph & Dagneu, 2019; Kan-In & Khunrattanasiri, 2020; Maury & Sharma, 2020; Sakthivel et al., 2021; Padmaja & Giridhar, 2022). Nearly all the earlier research works in Iraq have concentrated either on present or on historical LU/LC variations, and there has been limited research work on the prediction of spatial future LU/LC variations in the country (Mohammed, 2013; Omar et al., 2014; Al-Saady et al., 2015; Alzamili et al., 2015; Alkaradaghi et al., 2018; Mustafa & Ismail, 2019). Thus, the current research aims to address the past, present, and future changes of LU/LC for the LZRC by CA-Markov simulation. The outputs would offer valuable materials for protection ecologists to defend the ecosystems integrity, city manager and policymakers.

Materials And Methods

Study area

Lesser Zab River Catchment (LZRC); is placed in Erbil governorate, the north-east of Iraq, upstream of Tigris River, and north-west Iranian lands. It placed within latitudes 35°00'00"-36°60'00" N and 43°20'00"-46°20'00"E longitudes, cover a drainage area of almost 20,000 km² (Mohammed & Scholz, 2018). The catchment is designated by high topographic relief, with altitude changing from 306 to 1356 m.a.s.l. (Mohammed & Scholz, 2016). Nearly 24% of the catchment area is located in Iran, and the rest is in Iraq, Figure 1. Lesser (Lesser/Little) Zab river or Al-Zab Al-Saqeer is the major tributary of the Tigris River. Dokan, a multipurpose dam, was built in the Iraqi part of LZRC (35°57'14" N and 44°57'10" E), and Iran is lately constructing one and designing two more.

The catchment has a semi-arid continental climate in the north and north-east parts and an arid climate in the south and south-east parts with hot summer, occasionally, the maximum temperature reaches 42.2 °C and cool, wet winter (Mahdi & Mohammed, 2022). In that order, annual average air temperatures might range between 25.2 °C and 13.9 °C. The north and east portions of the catchment are generally mountainous areas; therefore, the yearly rain is considerably greater compared to the plain west and south portions (375-724 mm).

Data availability

Landsat satellite images of three historic sequential years (1999, 2010, and 2021) have been considered in the current research. The imagery scenes, of 30 m areal resolution and the minimum raincloud protection proportion, were obtained after the USGS (USGS, 2022) Earth Explorer portal (<https://earthexplorer.usgs.gov>), Table 1. After mosaicking the image parts of identical time frames and years, the area has been extracted. After that, and to correctly detect surface topographies before creating exercise data or spectral signature data for the organization, different band combinations have been exhibited, such as RGB 5, 4, 3 for OLI and RGB 4, 3, and 2 for TM. Before defining the scene feature classes depending on the training samples, historical and recent skilled information on the study area physiography, and valuable auxiliary records have been considered, for each LU/LC class recognized. Specifically, forest, agricultural land, plantation, urban area, barren land/dark, barren land/light and water body, Table 2, about 200 exercise trials in small polygons layout have resulted from the mosaicked imageries per required year (Lin et al., 2018). To classify each consecutive year image, the maximum likelihood method was used. Consecutively, three LU/LC maps with a spatial resolution of 30 m were produced.

Classification valuation

It is vital to measure the degree of agreement between automatic classification; with reference data (Li et al., 2018). An autonomous data comprising 30 per cent of the exercise data per class, for example, 30 per

cent of the 200 spectral autograph trials for every feature class equal to 60 points, was achieved by the ArcMap tool (Khwarahm et al., 2021b). The accuracy of 1999, 2010, and 2021 LU/LC maps, which resulted from the maximum likelihood method, were assessed by employing that dataset. A matching arbitrary sampling procedure was applied by producing 198 points scattering through every LU/LC map for every year. The 198 random points denote 34 points for water bodies class, 31 points for forest lands class, 35 points for agricultural lands class, 33 points for barren lands/dark class, 35 points for bare lands/light class, and 30 points for urban lands class for the categorized data (Gidado et al., 2019). Then, these points were transferred as shapefiles into Google Earth's historic images (reference plan) to be recognized and considered. To create an error matrix, the labelled points have been transferred back to the ArcMap tool (Hishe et al., 2021; Sakthivel et al., 2021). After that, producer and user accuracy; and the whole Kappa index of the agreement were calculated, depending on the error matrix. The quantification of the changing aspects of modification; during the time was then explored by computing the zone of specific classification each time frame (i.e., every year 1999, 2010, and 2021) (Juliev et al., 2019) after evaluating the produced LU/LC map's accuracy between 1999 and 2021.

C Cellular automata-markov chain simulation

Markov chain is one of the commonly known simulations to measure the degree of alteration during time through functioning the changing likelihood (transition probability) matrix, transition area matrix between t_0 and t_1 use/land cover time period maps (binary). Based on these matrices and their pixel-wise status, some restricted probability class classifications are expected (Khwarahm et al., 2021b). Although the Markov model is verified capable of mimicking the LU/LC modification (Cui et al., 2021; Hyandye & Martz, 2017). Still, the model is inadequate in mimicking the areal circulation of the class classifications in the LU/LC maps (Omar et al., 2014).

Alternatively, the Cellular Automata (CA) model (Khwarahm et al., 2021b) fills the gap of the spatial dimension constraint. Based on pre-defined conversion situations over time, the CA model calculates the LU/LC class classification new status built on the previous LU/LC status and those of its adjacent class classifications (Omar et al., 2014; Li et al., 2018; Kan-In & Khunrattanasiri, 2020). Integrating Markov chain simulation with the CA model delivers a distinctive prospect to calculate and simulate the spatiotemporal alteration of LU/LC regularly. This interaction model is capable of predicting and simulating difficult LU/LC classes (Hyandye & Martz, 2017). The CA-Markov model has been applied to predict LU/LC alteration during 2041, based on the (1999–2010) and (2010–2021) and the maximum likelihood classification, Fig. 2. This was achieved by the following main steps. Firstly, the maps of built-up and non-built-up areas were arranged and loaded into the ArcGIS 10.7 software. The maps of land use for the years 1999, 2010, and 2021 were re-classified to suit the objective of predicting urban development in LZRC. The land use maps were converted from vector to raster and then to ASCII files using conversion tools within the ArcGIS environment. Then, the IDRISI_Selva environment was used to re-classified and convert the ASCII files to a raster format. Accordingly, they can be considered to predict prospect urban

development. Markov chain model was applied to identify the transition probability matrix and transition rules for land use and land cover. Accordingly, the future LU/LC alteration was modeled, i.e., the transition probabilities for 1999 to 2010 were applied to predict the variations in 2021 and to calibrate and validate the model. Meanwhile, urban and non-urban maps of 2010 and 2021 were considered to predict future urban development in 2041. Markov simulation was firstly applied to produce transition probability matrices of zones and therefore conditional probability images for (1999–2010) and (2010–2021) LU/LC maps, in that order, Fig. 2. Model settings allowable just 15% related error for input imageries is suggested (Sakthivel et al., 2021). Secondly, a map of LU/LC for 2021 was modeled by the probability of transition and conditional images as input to the CA-Markov simulation. Then, to calibrate the model, the resulted image was validated with the real 2021 image. Next, a 2041 LU/LC map was simulated from the present (2010–2021) maps.

Model validation

It is essential to authorize the results of the model before simulating the LU/LC map for 2041. The validation was achieved by using an internal frame of the categorized data as reference data (categorized 2021 LU/LC image) compared to the modeled LULC map of 2021. IDRISI 17.0 has a fixed VALIDATE module that was used to compare the degree of the agreement between the classified and the modeled image. The agreement catalogues are founded on the typical KIA (Kappa Index of Agreement with particular areal relationship differences, which namely include; $K_{\text{locationStrata}}$ (Kappa for location Strata), K_{location} (for location), K_{no} (for no data), and K_{standard} (standard) (Viera & Garrett, 2005; Khwarahm et al., 2021a; Khwarahm et al., 2021a; Yi et al., 2022). Kappa locationSrata and location specify the aerial extents precision of the extent and positions of the grid-cells of a definite class classification of the LU/LC images. Kappa no, designates the overall agreement between the reference and simulated images parts, irrespective of having data on the amount and position of definite class categories. Kappa standard signifies the ratio of properly relating a class category compared to the ones that are linked properly through accidental. The values of Kappa for these differences vary from 0 to 1; the nearer the number to 1, the well is the agreement precision (Khwarahm et al., 2021a).

Results And Discussion

Assessment of the classification

Error matrices were considered to assess the accuracy of the maximum likelihood cataloguing, Tables 4 and 5. The agreement whole Kappa index for the three considered, 1999, 2010, and 2021 were 0.90 (90%), 0.95 (95%), 0.85 (85%), correspondingly. The user's and producer's precisions for every class classification were varied between 0.87 and 1.00 (Tables 3), which designate that the figure of pixels properly categorized in Google Earth. Historical images and local understanding of the catchment extent's physiography were suitable for correctly mining class classes. General, six class groups were recorded from the Landsat images, which recorded throughout the initial and late July of 1999, 2010, and 2021.

Alteration figures established between 1999 and 2010, the dense vegetation, bare lands, agricultural lands, urban lands, and water bodies have increased by 5.52, 3.45, and 0.19%, respectively, Table 4. These alterations are comparative concerning the total cover of the land categories between the two periods. The expansion in the urban area between 1999 and 2010 (11 years) is moderate. However, one may reflect on the instability of the financial and the essential circumstances in that period. The battle between Iran and Iraq, which lasted eight years, was just stopped in 1988; the gulf battle was happening and followed by the economic agreements of the United Nations. The expansion in bare lands may denote restricted farming action by agriculturalists in 2010, or the terrestrial has been recorded.

The increase in the density and magnitude of the forest areas; in the remote high lands; is revealed in Figure 5. Remarkably, the water bodies raised from 95.4 km² to 132.9 km² (0.2). However, agricultural land, barren lands/dark and light have decreased by 8.15, 0.4, and 0.78%, respectively. Between 2010 and 2021, change statistics established agricultural land, bare lands dark and bare lands light have reduced by 0.96, 0.28, and 1.23%, in that order. However, the urban area, forest and water bodies increased by 0.82, 1.57 and 0.04%, respectively. Through that period, the bare land displayed a constant reduction of about 11.9% of the entire area, while the extent of the built-up land raised from 240 to 1118 km², Table 4. The growth of the urban area denotes the growth of the population and expansion of the organizations (Khwarahm et al., 2021a). Population development is considered one of the main factors that cause LU/LC alterations (Wang & Zheng, 2022). Over the past two eras, Iraq has seen substantial population development and limited economic progress (UN, 2017).

Model validation

The actual LU/LC map of 2021 has been used to validate the modelled map of 2021. Generally, there was an excellent degree of fitting between the simulated and real images, Table 5. The overall Kappa numerical differences of $K_{no} = 0.8635$, $K_{location} = 0.8541$, $K_{location\ Strata} = 0.8541$, and $K_{standard} = 0.7853$ were accomplished, which are measured suitable to the extent that the model justification consistency is concerned for more use (Khwarahm et al., 2021a). The model is implemented reasonably in expecting the water bodies, bare land, urban areas, cultivated lands, and forest lands, Table 4. Yet, the model has overestimated the barren lands and agricultural lands by 2.73 (6990 km²) and 8.28 (7992 km²), and water bodies by 0.22 (90 km²), respectively of the actual area. In contrast, the model has underestimated the forest and urban land by 7.01 (3810 km²) and 4.22 % (1118 km²) of the actual land, respectively.

The underestimation most possible resulted from the disagreement amount assessment, Table 5, which has, to some extent, affected the total model performance. Additionally, the difference between the classified and the modelled LU/LC map of 2021 has resulted from underestimating specific class classifications, mainly farming bare and urban areas, Table 5. As there is an evident interval variance from 2010 to 2021, during which the speed and number of LU/LC alteration dynamics have altered associated with the period from 1999 to 2010. Conversely, the total model performance in modelling a prospect

scenario depending on the transition probability matrix of 1999–2010 established dressed precision, Table 5 and Fig. 3. Earlier research within the study region has stated several Kappa coefficient difference values for the CA-Markov method. For example, Khwarahm et al., 2021a reported the $K_{no} = 0.8339$, $K_{location} = 0.8222$, $K_{standard} = 0.7491$, in that order. Fig. 3 demonstrated that there is a good agreement between the anticipated and classified LU/LC maps with a coefficient of determination value of $R^2 = 0.95$, Fig. 3. This outcome agrees with the outcome of the (Khwarahm et al., 2021a) study, which stated that the $R^2 = 0.98$ between actual and predicted LU/LC maps.

LULC change modeling

The classified LU/LC maps for the 1999–2010 and 2010–2021 were considered to model 2021 and 2041 LU/LC maps, in that order. The results of LU/LC maps prediction revealed that between 2021 and 2041 urban areas would increase by 364.79% (from 1117.1 to 5192.2 km²). However, bare lands/light, agricultural lands, water bodies, bare lands/dark, and forest lands would decrease by 3% (from 6921.34 to 6723.70 km²), 12% (from 7972.85 to 7023.60 km²), 15% (from 141.03 to 119.86 km²), 30 (from 4.80 to 3.37 km²), and 76 (from 3808.86 to 903.20 km²), in that order, Table 5 and Fig. 4. These alterations (increases/declines) are comparative variations with respect to LU/LC class classifications. For example, a 365% increase in the urban area during 2041 would be at the cost of decreasing other class categories extent.

Additionally, variations ration in each class category area during the period from 2021 to 2041 designated that the maximum active class cover categories were urban lands, forest lands, and bare lands/dark. While, the least dynamic cover types were water bodies, agricultural lands, and bare lands/light. In 2041, the area of the bare lands/light would decline by only 3%, while the forest lands area with greater than 76.27% with respect to other land cover categories, Fig. 4. The utmost substantial alteration that balances out the total activity of the class classifications will be the agricultural lands and bare lands/light. These classes cover a significant area in comparison to the other classes. This result shows that particular zones, which were enclosed by water bodies in 2021, will be changed by urban lands, sequentially, further water bodies will arise. The appearance of water bodies will be utmost possibly be in the arrangement of catchments and minor scale lakes from fishery events, Figs. 5 and 6.

Conclusions

Lesser Zab River is one of the main Tigris River tributaries. The catchment of the Lesser Zab River is considered one of the essential biodiversity hot spots in the Kurdistan Region/Iraq. During the past 15 years, the croplands of the region has been altering at a linear speed. Developing procedures to measure spatially historical, present, and prospect alterations make available helpful material for policy-makers; and biodiversity ecologists and support in detecting environmentally degraded zones regarding the landscape's overall variety. For predicting the dynamics of LU/LC classes during 2040, the current study

has applied a combined method of GIS, remote sensing, and CA-Markov (earth surface modeller). Integrating remote sensing with GIS provides an excellent chance to monitor and measure LU/LC spatiotemporal variations regularly. Since 1999, there have been substantial variations in LU/LC, especially in urban areas, mainly in the neighbourhoods of the chief highways and near, west, south-east, and south-west of the metropolitan. Agricultural lands in the catchment have revealed a notable drop from 1999 to 2021, and future predictions established that this tendency would remain (i.e. from 2021 to 2041). Administration actions should emphasis protecting the agricultural zones as part of the ecological expansion. Besides, the more active LU/LC kind that raised the greatest over the last two decades was an urban area, which increased by four times from 1.20 to 5.59% from 1999 to 2021. Future predictions demonstrated that this trend would continue to increase from 5.59% (2021) to 26.01% (2041) (i.e. by almost four times). Urban areas would continue to expand mainly at the cost of agricultural, barren and forest areas. The results of this study offer vigorous reference point material for prospect use of the land surface landscapes with less effect on biodiversity and land reliability. The map of 2041 would be used as a standard for decision making, preparation, ecological management of the atmosphere, and biodiversity protection.

Declarations

All authors have read, understood, and have complied as applicable with the statement on "Ethical responsibilities of Authors" as found in the Instructions for Authors and are aware that with minor exceptions, no changes can be made to authorship once the paper is submitted.

Ethical Approval Not applicable

Consent to Participate Not applicable

Consent to Publish Not applicable

Authors Contributions Ruqayah Mohammed introduced the main idea, aim and objectives, discussed the obtained results, wrote and revised the manuscript. Zahra Ali Mahdi pledged the data collection and analysis and discussed part of the results.

Funding This research was not externally sponsored. This research did not receive any specific grant from funding agencies in the public, commercial or not-for-profit sectors.

Competing Interests Not applicable

Availability of data and materials The data sources have been mentioned under the Materials and Methods section

Acknowledgements The authors acknowledge the support of their particular organizations. The current study did not get any particular funding from finance organizations in the community, profitable or not-for-profit zones.

References

Alkaradaghi, K., Ali, S. S., Al-Ansari, N., & Laue, J. (2018). Evaluation of land use & land cover change using multi-temporal Landsat imagery: a case study Sulaimaniyah Governorate, Iraq. *Journal of Geographic Information System*, 10(3), 247–260. <https://doi.org/10.4236/jgis.2018.103013>

Alzamili, H. H., El-Mewafi, M., & Beshr, A. M. (2015). Monitoring urban growth and land use change detection with GIS and remote sensing techniques in Al-Nasiriyah city in Iraq. *International Journal of Scientific and Engineering Research*, 6(7), 2229– 5518

Cui L., Zhao Y., Liu J., Wang H., Han L., Li J., & Sun Z. (2021). Vegetation Coverage Prediction for the Qinling Mountains Using the CA–Markov Model. *ISPRS International Journal of Geo-Information*, 10(10), 679

Degife, A., Worku, H., Gizaw, S., & Legesse, A. (2019). Land use land cover dynamics, its drivers and environmental implications in Lake Hawassa Watershed of Ethiopia. *Remote Sensing Applications: Society and Environment*, 14, 178–190. <https://doi.org/10.1016/j.rsase.2019.03.005>

Dibaba, W. T., Demissie, T. A., & Miegel, K. (2020). Drivers and implications of land use/land cover dynamics in Finchaa catchment, northwestern Ethiopia. *Land*, 9(4), 113. <https://doi.org/10.3390/land9040113>

Gidado K. A., Kamarudin M. K. A., Hammad M., Ghurah S. A., Wahab N. A., Saad M. H. M., & Potikengrith T. (2019). Application of Ca-Markov Model for the Analysis of Urban Growth in Kenyir Catchment. *International Journal of Academic Research*, 9(2), 449–458

Hailu, Y., Tilahun, B., Kerebeh, H., & Tafese, T. (2018). Land use land cover change detection in Gibe Sheleko National Park, Southwestern Ethiopia. *Agricultural and Resource Economics: International Scientific E-Journal* 4(1868–2019–381), 20–30. <https://doi.org/10.22004/ag.econ.281757>

- Hishe S., Bewket W., Nyssen J., & Lyimo J. (2020). Analysing past land use land cover change and CA-Markov-based future modelling in the Middle Suluh Valley, Northern Ethiopia. *Geocarto International*, 35(3), 225–255
- Hyandy C., Martz L. W. (2017). A Markovian and cellular automata landuse change predictive model of the Usangu Catchment. *International Journal of Remote Sensing*, 38, 64–81
- Juliev, M., Pulatov, A., Fuchs, S., & Hübl, J. (2019). Analysis of Land Use Land Cover Change Detection of Bostanlik District, Uzbekistan. *Polish Journal of Environmental Studies*, 28(5). <https://doi.org/10.15244/pjoes/94216>
- Kan-In, K., & Khunrattanasiri, W. (2020). *Comparative Study on CA-Markov Model and CLUE-S Model for Land Use Changed Prediction in National Reserved Forest, Nan Province* (Doctoral dissertation, Kasetsart University).
- Khwarahm, N. R., Najmaddin, P. M., Ararat, K., & Qader, S. (2021a). Past and future prediction of land cover land use change based on earth observation data by the CA–Markov model: a case study from Duhok governorate, Iraq. *Arabian Journal of Geosciences*, 14(15), 1-14
- Khwarahm, N. R., Qader, S., Ararat, K., & Al-Quraishi, A. M. F. (2021b). Predicting and mapping land cover/land use changes in Erbil/Iraq using CA-Markov synergy model. *Earth Science Informatics*, 14(1), 393–406. <https://doi.org/10.1007/s12145-020-00541-x>
- Lin, X., Xu, M., Cao, C., Singh, P. R., Chen, W., & Ju, H. (2018). Land-use/land-cover changes and their influence on the ecosystem in Chengdu City, China during the period of 1992–2018. *Sustainability*, 10(10), 3580. <https://doi.org/10.3390/su10103580>
- Maury, C., & Sharma, V. N. (2020). *Land use/Land cover Change Detection in Auranga River Basin, Jharkhand*
- Mohammed, J. (2013). Land use and cover change assessment using Remote Sensing and GIS: Dohuk City, Kurdistan, Iraq (1998–2011). *International journal of Geomatics and Geosciences*, 3(3), 552
- Mohammed, R., & Scholz, M. (2016). Impact of climate variability and streamflow alteration on groundwater contribution to the base flow of the Lesser Zab River (Iran and Iraq). *Environmental Earth Sciences*, 75(21), 1–11. <https://link.springer.com/article/10.1007/s12665-016-6205-1>
- Mohammed R., & Scholz M. (2018). Climate change and anthropogenic intervention impact on the hydrologic anomalies in a semi-arid area: Lesser Zab River Catchment, Iraq. *Environmental Earth Sciences*, 77(10), 1–19. <https://link.springer.com/article/10.1007/s12665-018-7537-9>
- Mahdi Z. A., & Mohammed R. (2022). Land use/land cover changing aspect implications: Lesser Zab River Basin, northeastern Iraq. *Environmental Monitoring and Assessment*, 194(652), 1-16. <https://doi.org/10.1007/s10661-022-10324-0>

- Msofe, N. K., Sheng, L., & Lyimo, J. (2019). Land use change trends and their driving forces in the Kilombero Valley Floodplain, Southeastern Tanzania. *Sustainability*, 11(2), 505. <https://doi.org/10.3390/su11020505>
- Munthali M. G., Mustak S., Adeola A., Botai J., Singh S. K., & Davis N. (2020). Modelling land use and land cover dynamics of Dedza district of Malawi using hybrid Cellular Automata and Markov model. *Remote Sensing Applications: Society and Environment*, 17, 100276
- Mustafa, Y. T., & Ismail, D. R. (2019, April). Land use land cover change in Zakho District, Kurdistan Region, Iraq: past, current and future. In *2019 International Conference on Advanced Science and Engineering (ICOASE)* (pp. 141–146). IEEE.
- Oliver T. H., & Morecroft M. D. (2014). Interactions between climate change and land use change on biodiversity: attribution problems, risks, and opportunities. *Wiley Interdisciplinary Reviews: Climate Change*, 5(3), 317–335. <https://doi.org/10.1002/wcc.271>
- Omar N. Q., Ahamad M. S. S., Wan Hussin W. M. A., Samat N., & Binti Ahmad S. Z. (2014). Markov CA, multi regression, and multiple decision making for modeling historical changes in Kirkuk City, Iraq. *Journal of the Indian Society of Remote Sensing*, 42(1), 165–178
- Padmaja, G., & Giridhar, M. V. S. S. (2022). Utility of Geomatics in Land Use Land Cover Change Detection and Accuracy Analysis. In *Advanced Modelling and Innovations in Water Resources Engineering* (pp. 517–527). Springer, Singapore
- Sakthivel, M., Priyadharshini, J., & Vijayakumar, S. (2021). Accuracy Assessment of Land Use Land Cover Classification using GIS and Remote Sensing Approach: A Case Study of Tiruchirappalli District, Tamil Nadu, India. *The International journal of analytical and experimental modal analysis*, XIII(VIII), 861–875. <https://doi.org/10.4236/ijg.2017.84033>
- Saleh, A. M., & Ahmed, F. W. (2021). Analyzing Land Use/Land Cover Change Using Remote Sensing and GIS in Mosul District, Iraq. *Annals of the Romanian Society for Cell Biology*, 4342–4359. <https://www.annalsofrscb.ro/index.php/journal/article/view/1928>
- Shteiwi, M. E., Zarzoura, F., & Jumaah, Z. (2021). A Comparative Study of the different remote sensing techniques for evaluating land use/cover in Basra city, Iraq.(Dept. C). MEJ. *Mansoura Engineering Journal*, 45(4), 21–32. <https://dx.doi.org/10.21608/bfemu.2021.139429>
- UN, World Environment Day (2013). *How environmental damage causes food insecurity in Iraq*. Retrieved March 31 2020, from <https://reliefweb.int/sites/reliefweb.int/files/resources/Factsheet-WorldEnvironment-English.pdf>
- UN (2017). *Department of economic and social affairs, population division*. World population prospects: The 2017 revision, Volume II: Demographic Profiles. ST/ESA/SER.A/400

USGS .*United States Geological Survey, Earth Explorer portal*. Retrieved January 9 2022, from <https://earthexplorer.usgs.gov>

Viera, A. J., & Garrett, J. M. (2005). Understanding inter observer agreement: the kappa statistic. *Family Medicine*, 37(5), 360–363. PMID: 15883903.

Wang L., Yu D., Liu Z., Yang Y., Zhang J., Han J., & Mao Z. (2018). Study on NDVI changes in Weihe Watershed based on CA–Markov model. *Geological Journal*, 53, 435–441

Wang S., & Zheng X. (2022). Dominant transition probability: combining CA-Markov model to simulate land use change. *Environment, Development and Sustainability*, 1–19

Yesuph, A. Y., & Dagne, A. B. (2019). Land use/cover spatiotemporal dynamics, driving forces and implications at the Beshillo catchment of the Blue Nile Basin, North Eastern Highlands of Ethiopia. *Environmental Systems Research*, 8(21), 1–30. <https://doi.org/10.1186/s40068-019-0148-y>

Yi S., Zhou Y., & Li Q. (2022). A New Perspective for Urban Development Boundary Delineation Based on the MCR Model and CA-Markov Model. *Land*. 11(3), 401

Tables

Table 1 Sensor and date/time of the scene acquisitions from Landsat 5 Thematic Mapper (TM) and Landsat 8 (OLI_TIRS)

Path	Row	Date/time (Sensor_TM)	Date/time (Sensor_TM ^a)	Date/time (Sensor_OLI ^b _TIRS ^c)
168	35	20.7.1999 (TM)	02.7.2010 (TM)	16.7.2021 (OLI)
168	36	20.7.1999 (TM)		16.7.2021(O LI)
169	35	27.7.1999 (TM)	09.7.2010 (TM)	23.7.2021(O LI)
169	36		09.7.2010 (TM)	23.7.2021(O LI)
170	36			30.7.2021(O LI)

Path/row=168/35, 168/36, 169/35, 169/36, 170/35, 170/36

Note: spatial resolution of 15m is used for the panchromatic band 8 for Landsat 8

^aThematic Mapper; ^bOperational Land Image; ^cOperational Land Image and Thermal

Table 2 Description of the land use/land cover classes

Class	Description
Forest	Very densely vegetated areas, mostly forest and dense shrub lands.
Agricultural land	Presently cropped area with noticeable greenness
Urban area	Synthetic Structure
Bare land/light	Lands with no apparent/or negligible plants, specially no evident covers of trees or shrubs, wasteland, rocky mounts and bare open lands
Bare Land/dark	Lands with no evident/or negligible plants, particularly no noticeable covers of trees or plants. Rocky mounts, bare rocks, hills, and soil
Water bodies	Any water bodies such as rivers, lakes, and fishponds

Table 3 Transition probability matrix resulting from land use maps for the period from 1999 to 2010 and 2010 to 2021

Matrix 2021						
1999	2010					
	WB ¹	FL ²	AL ³	BLD ⁴	BLL ⁵	UL ⁶
WB ¹	0.8010	0.1989	0.0000	0.0000	0.0000	0.0001
FL ²	0.0031	0.5669	0.3796	0.0040	0.0248	0.0215
AL ³	0.0041	0.2721	0.5106	0.0068	0.1617	0.0446
BLD ⁴	0.0085	0.2447	0.2358	0.0677	0.4078	0.0356
BLL ⁵	0.0001	0.0618	0.1345	0.0040	0.7384	0.0612
UL ⁶	0.0123	0.1408	0.2614	0.0056	0.3753	0.2047
O _v [*]	91.81 (1999)					
K _a ^{**}	90.08					
Matrix 2041						
2010	2021					
	WB ¹	FL ²	AL ³	BLD ⁴	BLL ⁵	UL ⁶
WB ¹	0.7659	0.1592	0.0330	0.0000	0.0087	0.0332
FL ²	0.0056	0.3359	0.4866	0.0002	0.1105	0.0613
AL ³	0.0009	0.3273	0.5445	0.0001	0.0934	0.0339
BLD ⁴	0.0003	0.1854	0.5716	0.0002	0.1952	0.0473
BLL ⁵	0.0001	0.0474	0.2778	0.0004	0.5636	0.1107
UL ⁶	0.0014	0.1411	0.3465	0.0003	0.2984	0.2123
O _v [*]	87.3 (2021)		91.8 (2010)			
K _a ^{**}	84.76		90.08			

¹Water Bodies, ²Forest lands, ³Agricultural land, ⁴Bare land/dark, ⁵Bare lands/light, ⁶Urban land; * Overall accuracy, ** Kappa Index

Table 4 Area and percentage of area of the land use land cover classes alteration

Class	Area									
	1999		2010		2021		2021 simulated		2041 simulated	
	(km ²)	(%)	(km ²)	(%)	(km ²)	(%)	(km ²)	(%)	(km ²)	(%)
WB ¹	128	0.64	104	0.52	90	0.45	134	0.67	120	0.60
FL ²	2394	11.97	3021	15.105	3810	19.05	2408	12.04	904	4.52
AL ³	9800	49	9001	45.005	7992	39.96	9648	48.24	7036	35.18
BLD ⁴	140	0.7	41	0.205	7	0.035	238	1.19	4	0.02
BLL ⁵	7298	36.49	7011	35.055	6983	34.915	7298	36.49	6736	33.68
UL ⁶	240	1.2	822	4.11	1118	5.59	274	1.37	5200	26.00
Total	20000	100	20000	100	20000	100	20000	100	20000	100

¹Water Bodies, ²Forest, ³Agrucultural Lands, ⁴Bare Lands Dark, ⁵Bare Lands Light, Urban Lands

Table 5 Coefficients of agreement between the real and modeled land use and land cover 2021 map

Classification agreement/disagreement

According to the ability to specify accurately quantity and allocation

Information of Allocation	Information of Quantity		
	No [n]	Medium [m]	Perfect [p]
$P(x)^1$	0.4996	0.9561	1.0000
$K(x)^2$	0.4996	0.9561	0.9980
$M(x)^3$	0.4163	0.8830	0.8851
$H(x)^4$	0.1429	0.4549	0.4542
$N(x)^5$	0.1429	0.4549	0.4542
Agreement Chance = 0.1429			
Agreement Quantity = 0.3120			
Agreement Strata = 0.0000			
Agreement Grid cell = 0.4281			
Disagree Grid cell = 0.0731			
Disagree Strata = 0.0000			
Disagree Quantity = 0.0439			
$K_{no} = 0.8635$			
$K_{location} = 0.8541$			
$K_{location} \text{ Strata} = 0.8541$			
$K_{standard} = 0.7853$			

¹Perfect, ²Perfect Stratum, ³Medium Grid, ⁴Medium Stratum, ⁵No

Figures

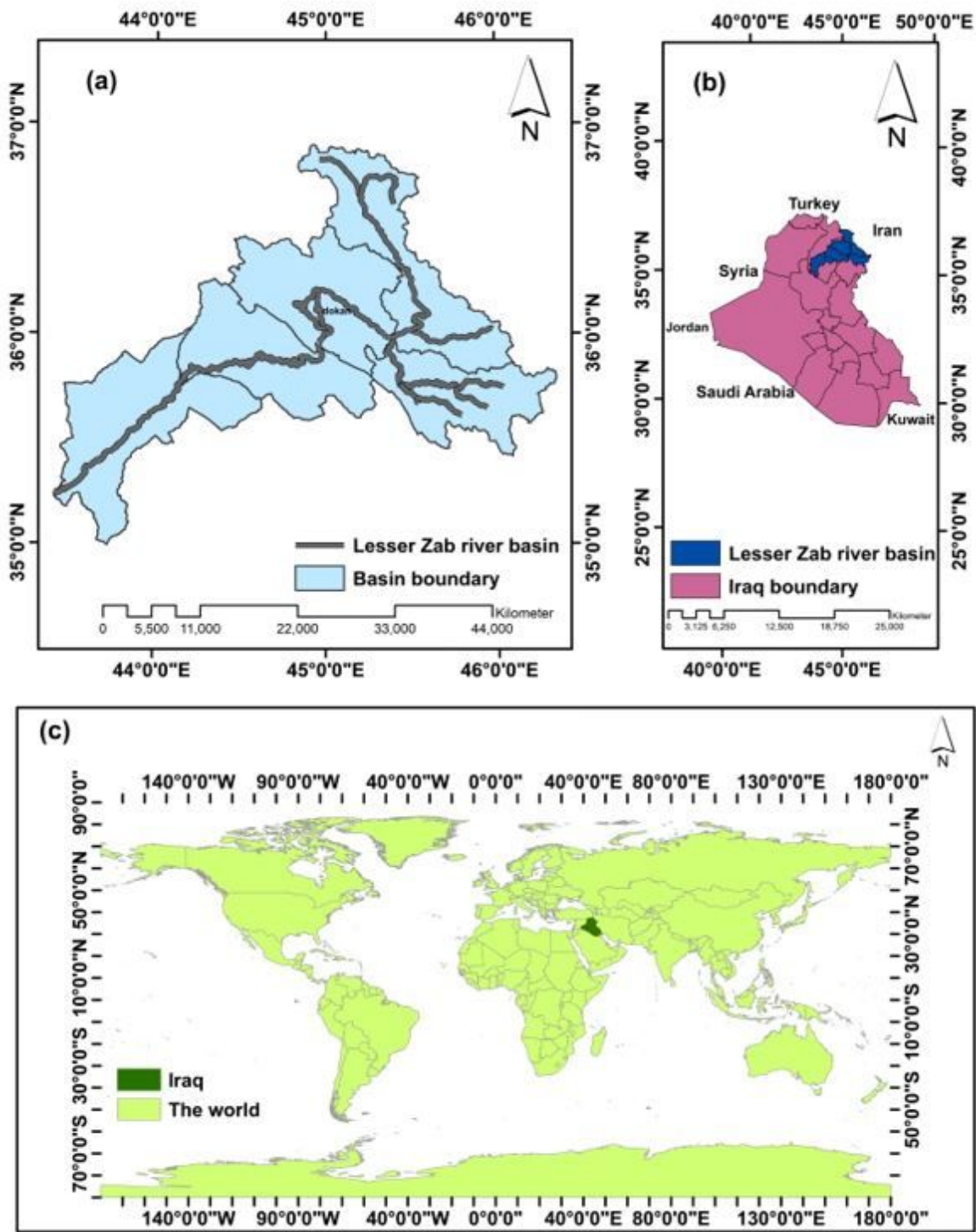


Figure 1

(a) The hydrographical system of the Lesser Zab River Catchment is located in (b) Iraq

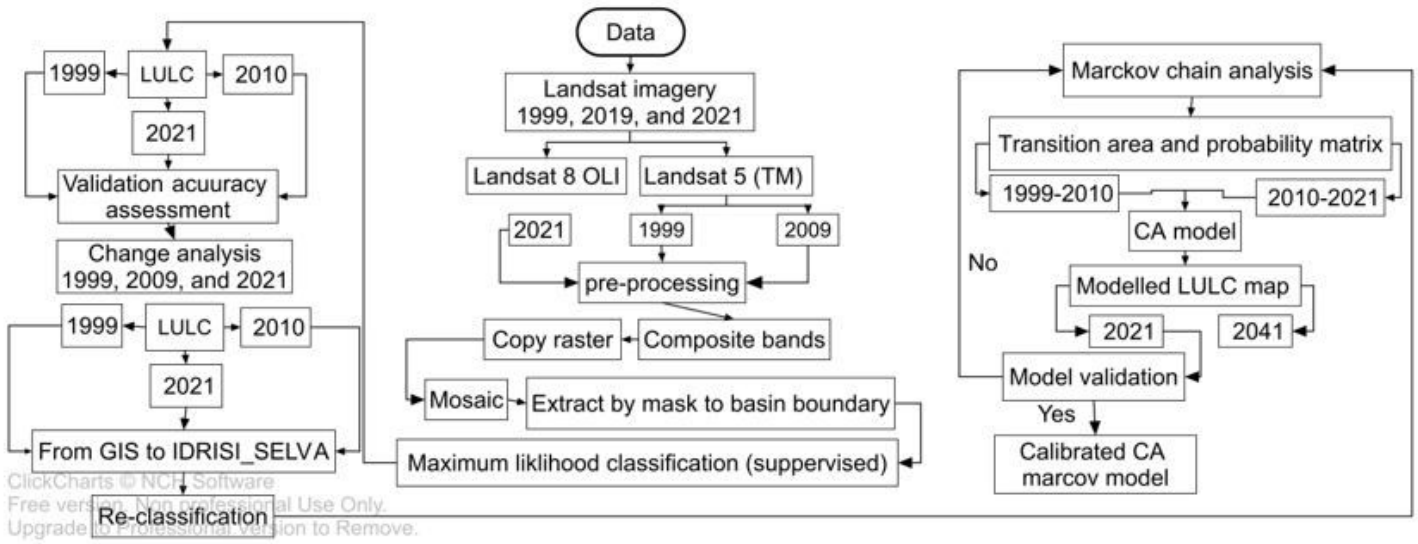


Figure 2

The applied methodology for assessing the implication of land use and land cover (LU/LC) alteration on the Lesser Zab River Catchment, Northeastern Iraq

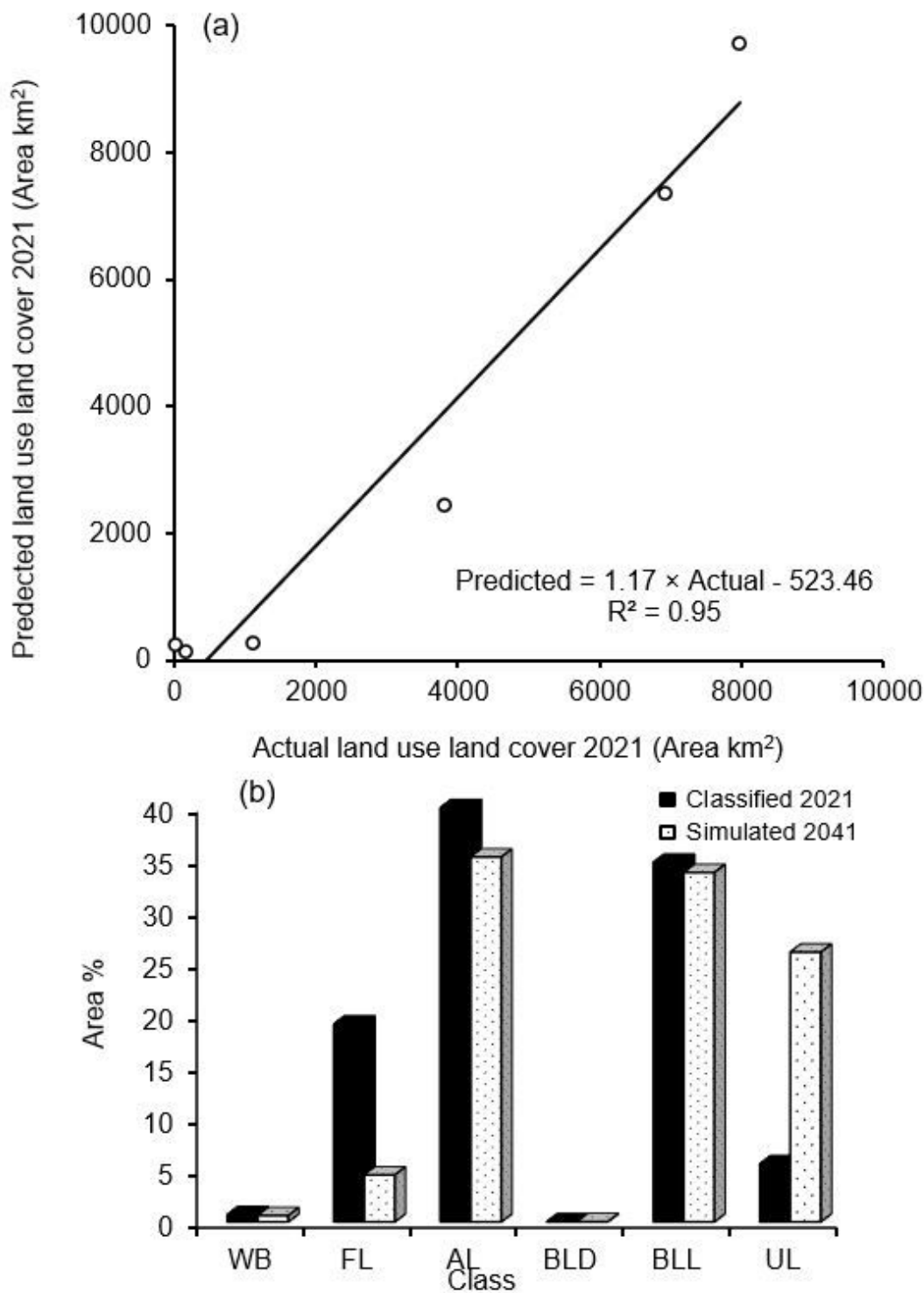


Figure 3

(a) The relationship between the actual and predicted land use and land cover maps of 2021; (b) Dynamics of land use/land cover for 2021 and 2041. Note: WB=Water Bodies, FL=Forest lands, AL=Agricultural land, BLD=Bare land/dark, BLL=Bare lands/light, UL=Urban land

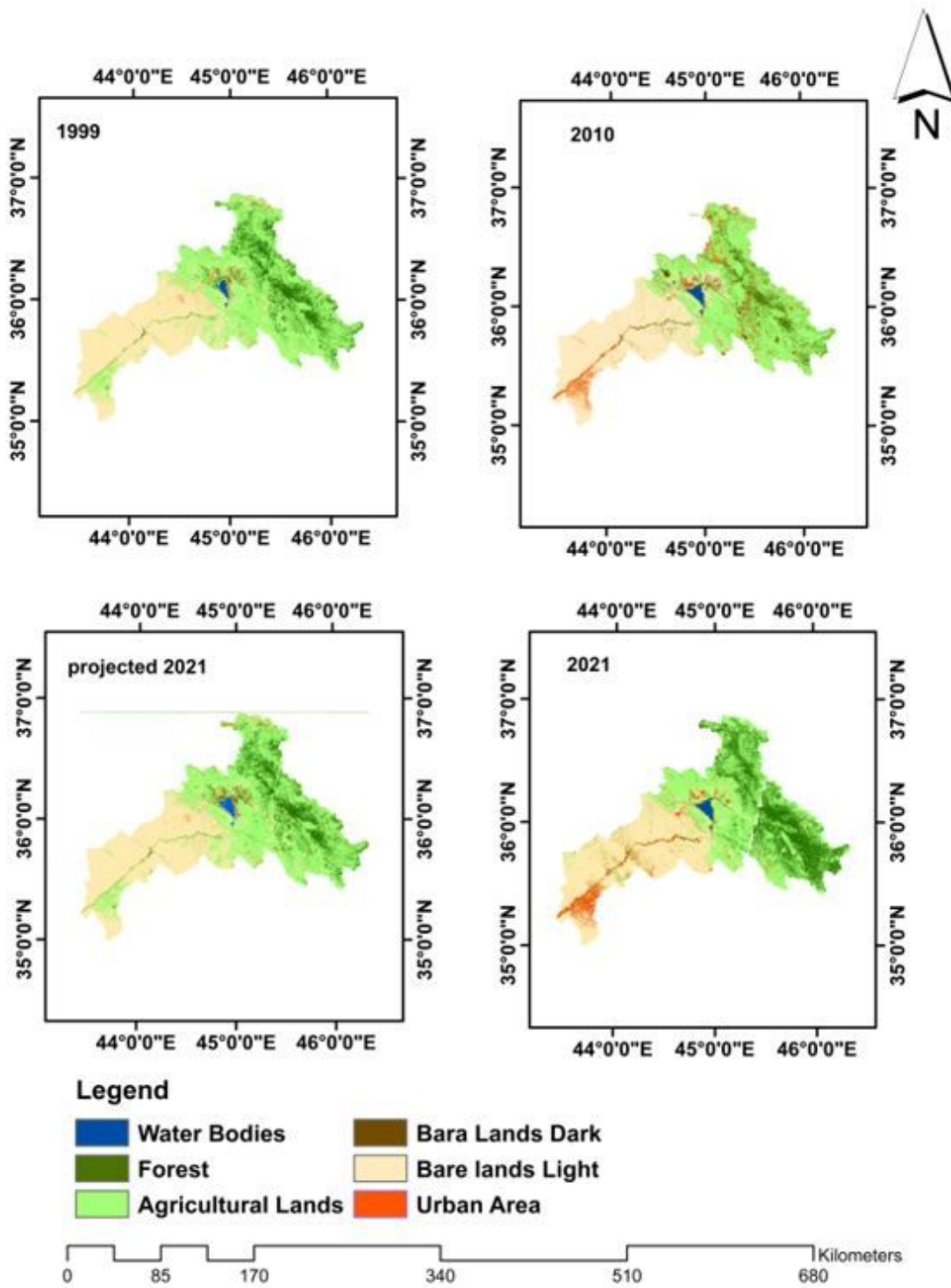


Figure 4

Land use/land cover maps for a) 1999, b) 2010, c) 2021, and d) simulated 2021

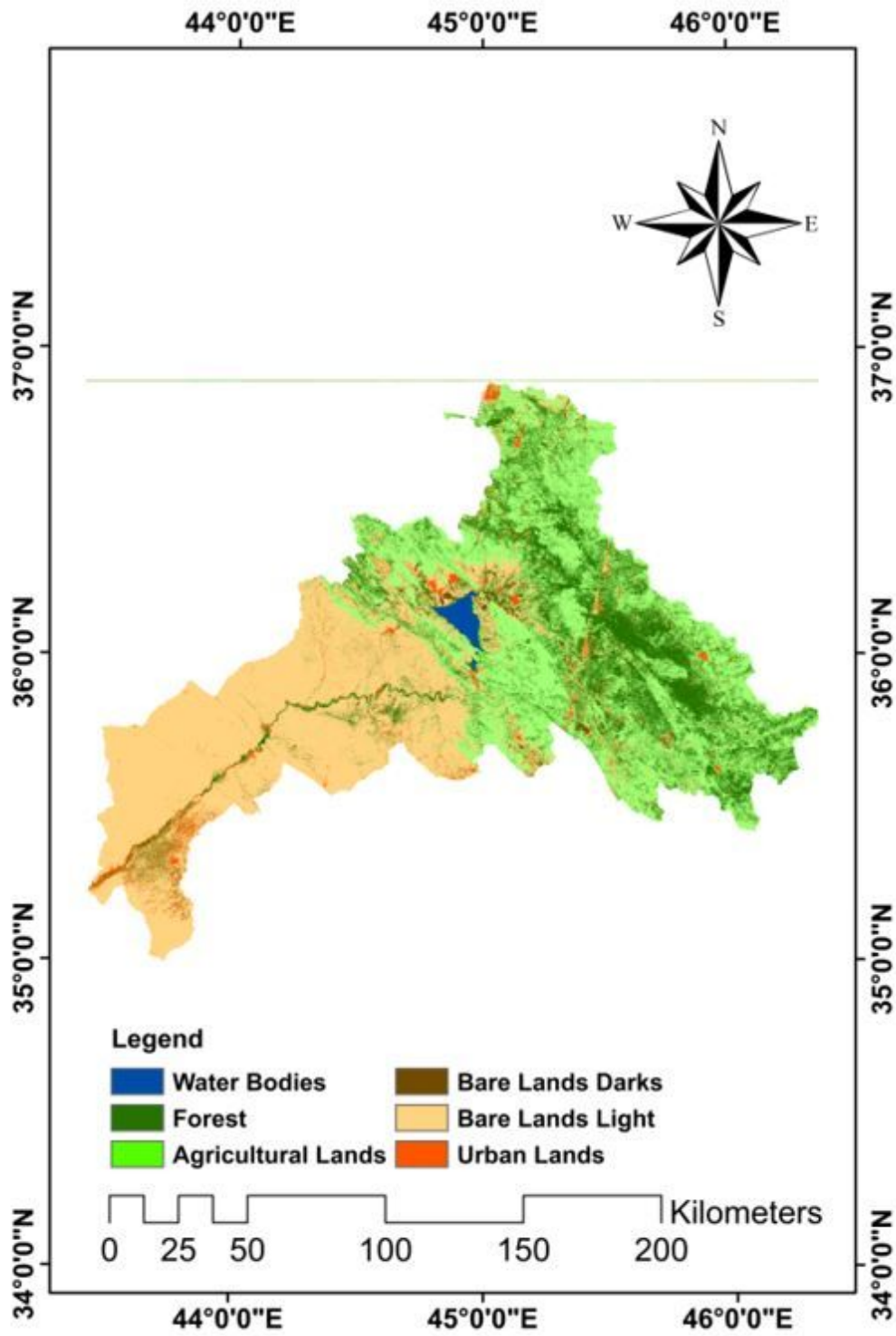


Figure 5

The simulated land cover and land use status of the Lesser Zab River Catchment for the 2041 year